The Class II KNOX transcription factors *KNAT3* and *KNAT7* *synergistically regulate monolignol biosynthesis* in *Arabidopsis*

Wenqi Qin[1,2], Qi Yin[1,2], Jiajun Chen[1,2], Xianhai Zhao[1,2], Fengxia Yue[3], Junbo He[1,2], Linjie Yang[3], Lijun Liu[4], Qingyin Zeng[5], Fachuang Lu[3], Nobutaka Mitsuda[6], Masaru Ohme-Takagi[7], Ai-Min Wu[1,2 *]

[1]State Key Laboratory for Conservation and Utilization of Subtropical Agro-bioresources, South China Agricultural University, Guangzhou 510642, China

[2]Guangdong Key Laboratory for Innovative Development and Utilization of Forest Plant Germplasm, College of Forestry and Landscape Architecture, South China Agricultural University, Guangzhou 510642, China

[3]State Key Laboratory of Pulp and Paper Engineering, South China University of Technology, Guangzhou 510640, China

[4]State Forestry and Grassland Administration Key Laboratory of Silviculture in downstream areas of the Yellow River, College of Forestry, Shandong Agriculture University, Taian 271018, Shandong, China

[5]State Key Laboratory of Tree Genetics and Breeding, Chinese Academy of Forestry, Beijing 100091, China

[6]Bioproduction Research Institute, National Institute of Advanced Industrial Science and Technology (AIST), Tsukuba 305-8566, Ibaraki, Japan

[7]Green Biology Research Center, Saitama University, Saitama 338-8570, Japan

[*]Correspondence: Ai-Min Wu (wuaimin@scau.edu.cn)

Highlights:

We demonstrate that KNAT3 and KNAT7 influence secondary cell wall deposition, KNAT3 and KNAT7 can form heterodimer and KNAT3 interacts with fiber-specific transcription factors NST1/2 to regulate syringyl lignin biosynthesis via influencing *F5H* gene expression.

ABSTRACT

The function of *KNOTTED ARABIDOPSIS THALIANA7 (KNAT7)* transcription factor is still unclear since it appears either as a negative or a positive regulator for secondary cell wall deposition with its loss-of-function mutant displaying thicker interfascicular and xylary fiber cell walls but thinner vessel cell walls in inflorescence stems. To explore the exact function of KNAT7, Class II KNOTTED1-like homeobox (*KNOXII)* genes including *KNAT3, KNAT4* and *KNAT5 were studied together. By chimeric repressor technology, we found that both KNAT3 and KNAT7 repressors exhibited a similar dwarf phenotype. Both KNAT3 and KNAT7 genes* were expressed in the inflorescence stems and the *knat3 knat7* double mutant exhibited a dwarf phenotype similar to the repressor lines. Stem cross-section of *knat3 knat7* displayed an enhanced irregular xylem phenotype as compared to the single mutants, and its cell wall thickness in xylem vessels and interfascicular fibers were significantly reduced. Cell wall chemical composition analysis revealed that syringyl lignin significantly decreased while guaiacyl lignin increased in the *knat3 knat7* double mutant. Coincidently, transcriptome of *knat3 knat7 showed that most lignin pathway genes were activated, whereas* syringyl lignin related gene *Ferulate 5-Hydroxylase* (*F5H*) was obviously downregulated. Protein interaction analysis discovered that KNAT3 and KNAT7 can form a heterodimer, and KNAT3, but not KNAT7, can interact with the key second cell wall formation transcription factors NST1/2, which suggests that the KNAT3 NST1/2 heterodimer complex regulates *F5H* to promote syringyl lignin synthesis. These results indicate that *KNAT3 and KNAT7* synergistically work together to promote secondary cell wall biosynthesis.

Keywords: KNAT3, KNAT7, xylem, secondary cell wall, complex, lignin

INTRODUCTION

Lignin is one of the major structural components in plant secondary cell walls and provides mechanical strength and stiffness to the plant cells (Boerjan *et al*., 2003; Cosgrove and Jarvis, 2012). Three types of lignin subunits i.e. *p*-hydroxyphenyl (H), guaiacyl (G), and syringyl (S) are derived from oxidative polymerization of three monolignols, *p*-coumaryl, coniferyl and sinapyl alcohols, respectively (Boerjan *et al.*, 2003).

Phenylalanine is used as substrate to produce hydroxycinnamoyl-CoA esters in the phenylpropanoid pathway involved in monolignol biosynthesis. At least eleven enzymes are involved in catalyzing monolignol biosynthesis including: phenylalanine ammonia lyase (*PAL*), cinnamate 4-hydroxylase (*C4H*), 4-coumarate CoA ligase (*4CL*), hydroxycinnamoyl CoA:shikimate hydroxycinnamoyl transferase (*HCT*), *p*-coumaroyl shikimate 3'-hydroxylase (*C3H*), caffeoyl CoA *O*-methyltransferase (*CCoAOMT*), *F5H*, caffeic acid *O*-methyltransferase (*COMT*), cinnamoyl CoA reductase (*CCR*), cinnamyl alcohol dehydrogenase (*CAD*) and caffeoyl shikimate esterase (*CSE*) (Boerjan *et al.*, 2003; Bonawitz and Chapple, 2010; Vanholme *et al.*, 2013). Of these enzymes, F5H is the key catalyst in the synthesis of S-lignin. A complicated transcriptional network regulates secondary cell wall formation, which contains the top-level regulators VASCULAR RELATED NAC-DOMAIN PROTEIN6 (VND6), VND7, and NAC (NAM, ATAF1/2, and CUC2) transcription factors, second-level regulators MYB46 and MYB83, and a battery of downstream transcription factors MYB20, MYB42, MYB43, MYB52, MYB54, MYB58, MYB63, MYB69, MYB85, MYB103, and KNAT7. The transcriptional regulation of lignin biosynthesis has revealed that some of MYB transcription factors can activate monolignol pathway genes directly by binding to the AC-rich elements of their promoters (Lacombe *et al.*, 2000; Patzlaff *et al.*, 2003; Goicoechea *et al.*, 2005; Zhou *et al.*, 2009). The promoters of *PAL*, *4CL*, *C3H*, *CCoAOMT*, *CCR* and *CAD* all contain the conserved AC elements while the promoters of *C4H* and *COMT* contain degenerated AC elements（Zhou *et al.*, 2009； Zhao *et al.*, 2011）. Therefore, all those genes might be directly regulated by the known lignin specific transcription factors, such as *AtMYB58* and *MYB63*. However, *F5H*, the key gene for S-lignin biosynthesis, neither contains AC-rich elements nor is regulated by the lignin-specific transcription factors (Zhou *et al.*, 2009; Zhao and Dixon, 2011). Although it is reported that the *Medicago F5H* gene is directly regulated by SND1

(NST3) (Zhao *et al.*, 2010), evidence for such regulation in *Arabidopsis* is lacking (Ohman *e,t al*., 2013). The molecular regulation of *F5H* in *Arabidopsis* is still elusive.

KNAT7, has been reported to function as a repressor of secondary cell wall formation, and disruption of it results in thicker interfascicular fiber walls in *Arabidopsis* (Li *et al.*, 2012). The known KNAT7 interactors, such as OVATE FAMILY PROTEIN4 (OFP4), BELL-LIKE HOMEODOMAIN6 (BLH6), and MYB75 (Hackbusch *et al.*, 2005; Bhargava *et al.*, 2010; Li *et al.*, 2011; Liu *et al.*, 2014) are negative regulators of secondary wall formation. Paradoxically, *knat7* mutant had thinner vessel cells (Li *et al.*, 2012), and reduced secondary wall thickness in dominant repressing transgenic plants of *KNAT7* (Zhong *et al.*, 2008). Our recent study revealed that KNAT7 positively affects xylan (the important composition of hemicellulose) biosynthesis (He *et al.*, 2018). These results imply that KNAT7 exhibits complicated functions on the specific cell types or interacting regulators.

KNAT7 is one of *KNOTTED1-LIKE HOMEBOX* (*KNOX*) genes, which belong to the plant-specific Three Amino Acid Loop Extension (TALE) homeodomain superfamily (Hake *et al.*, 2004; Hay and Tsiantis, 2010). *KNOX* genes can be grouped into two classes *KNOX I* (*SHOOTMERISTEMLESS* (*STM*), *BREVIPEDICELLUS* (*BP*), *KNAT2* and *KNAT6*) and *KNOX II* (*KNAT3*, *KNAT4*, *KNAT5* and *KNAT7*) (Kerstetter *et al.*, 1994; Mukherjee *et al.*, 2009). *KNAT3*, *KNAT4*, and *KNAT5* function redundantly to influence leaf morphology in *Arabidopsis* (Furumizu *et al.*, 2015). As *KNOX II* clade members, it would be interesting to explore whether *KNAT3*, *KNAT4* and *KNAT5* have redundant functions with *KNAT7* on secondary wall formation in inflorescence and stem thus to interpret the diverse and paradoxical roles of *KNAT7*.

Here, we report that the loss-of-function *knat3 knat7* double mutant displays an enhanced irregular xylem (*irx*) phenotype including thinner vessel and interfascicular cell wall thickness. The actual contents of the chemical composition revealed an increase in G-lignin and a decrease in S-lignin. RNA-seq results displayed significant downregulation of *F5H*. Protein interaction assay identified that KNAT3 and KNAT7 form heterodimer, and KNAT3, but not KNAT7, can interact with NST1 and NST2. Altogether, our results explain that KNAT3 and KNAT7 form a complex to paradoxically regulate secondary cell wall formation in different tissue.

MATERIALS AND METHODS

Plant material and growth conditions

Arabidopsis thaliana ecotype *Columbia* (Col‐0) was used as the WT plant and transgenic plant experiments. Plants were grown in a photoperiod with supplemental lights under 16-h-light/8-h-dark cycles and the light intensity and temperature were 120 µmol m^{-2} s^{-1} light and 22 °C on soil, respectively. The T‐DNA insertion mutant allele of *myb103-1* (AT1G63910 SALK_210187C), *myb103-2* (AT1G63910 SAIL_337_C03), *KNAT3* (AT5G25220 SALK_136464) and *KNAT7* (AT1G62990 SALK_110899), designated *knat3* and *knat7*, were identified using the SIGnal database (http://signal.salk.edu/) and seeds were obtained from the Arabidopsis Biological Resources Center (ABRC, Columbus, OH, USA). *KNAT3* and *KNAT7* gene-specific primers used for PCR genotyping are listed in Table S1.

Plasmid constructs and generation of transgenic plants

Promoter fragments of 2kb, 2.6kb upstream to the ATG start codons of *KNAT3* and *KNAT7* were designed. The promoter fragments were cloned into the pDONR207 vector and then transferred into pGWB3 (Nakagawa *et al.*, 2007) and all constructs were used to transform WT *Arabidopsis*. Both KNAT3 and KNAT7 coding regions were individually cloned into pDONR207 and then recombined into pEarleyGate100. Chimeric repressor constructs were prepared by inserting coding sequence of *KNAT3* and *KNAT7* with one extra guanine nucleotide at 5' end into SmaI site of p*35S*:SRDXG vector and then transferred into vector pBCKH (Mitsuda *et al.*, 2006), in which a chimeric repressor is produced by fusion transcription factors to the plant-specific ERF associated Amphiphilic Repression (EAR) repression domain (LDLDLELRLGFA). Finally, all DNA constructs were verified by DNA sequencing analysis and were electroporated into *Agrobacterium tumefaciens* GV3101. Transformation of WT plants and *knat3 knat7* double mutant was done using floral dipping method (Clough and Bent, 1998). Transgenic lines were screened on 1/2 MS plates plus 50 mg mL^{-1} kanamycin or 2000X Glufosinate ammonium (sigma).

GUS staining

GUS activity was examined in 40 mm sections of 6-week-old inflorescence stems. Sections were washed three times with PBS buffer (pH 7.0), and incubated with GUS staining solution (100 mM Na_3PO_4, pH 7.0, 1 mM EDTA, 1 mM potassium ferrocyanide, 1 mM potassium ferricyanide, 1% Triton X-100, and 1 mg/mL 5-bromo-4-chloro-3-indolylb-D-glucuronide (X-Gluc)) for 8h to overnight at 37°C in dark. After being decolorized in 95% or 75% ethanol (Jefferson *et al.*, 1987; Wu *et al.*, 2009), the sections were observed under light microscope.

Sectioning of Stems

Segments were cut from the basal internode of stems of 6-week-old plants. Leica VT1000S vibratome was used to cut 40 mm sections by using a 3% agarose as support. Phloroglucinol-HCl Staining was performed; the sections were stained for 5 sec in 3% phloroglucinol then were washed out, followed by the addition of concentrated HCl (37N) and then observed using a light microscope. For Mäule Staining, 0.5% potassium permanganate solution was added to the sections for staining. The solution was washed out and then distilled water was added to rinse out the potassium permanganate solution. Finally, 3% HCl was added and incubated for 3-5 min until the deep brown color was discharged from the sections. After pipetting out all the HCl solution, concentrated ammonium hydroxide solution was added immediately (Pradhan and Loque, 2014). Then the sections were observed under bright field of microscopy (BX43F; Olympus, Japan). Finally, cell wall thickness was measured by software within the microscope and combined with software image J.

Cell wall preparation and lignin analysis

To measure total lignin content and monomeric lignin composition, 8-week-old mature stems were collected with three biological replicates with each replicate having at least 6 plants. After ball-milled into powder, wax was removed using soxhlet extractor. The powders were incubated with 4% diluted sulfuric acid at 121 °C for 60-minutes to completely hydrolyze. The hydrolysate was filtered to determine the acid-soluble lignin, and the residue was measured for acid-insoluble lignin. Determination and calculation methods were the same as previously described (Wang *et al.*, 2019). Thioacidolysis was used to analyze lignocellulosic samples and 2D HSQC was performed following the methods used by (Yue *et al.*, 2012) and (Kim and Ralph, 2010; Mansfield *et al.*, 2012) respectively.

RNA-seq

Six-week-old *Arabidopsis* stem bases of Col-0 and *knat3 knat7* plants were collected and ground into powder in liquid nitrogen. Total RNA extraction and RNA-seq were performed by the Biomarker Technologies Corporation (Beijing China). Differential gene expression analysis and Gene Ontology enrichment analysis were performed using BMKcloud (international.biocloud.net). The TAIR10 genome was used as the *Arabidopsis* reference genome (www.arabidopsis.org) and the RNA-seq data was submitted to http://bigd.big.ac.cn/gsa/ with submission number: CRA002075.

RT-PCR and qRT-PCR analyses

Total RNA was isolated using a plant RNA kit (Omega, Norcross, GA, USA) according to the manufacturer's instructions. First-strand cDNA synthesis was carried out with approximately 2μg RNA using the Primer Script RT Reagent Kit with gDNA Eraser (Takara, Kyoto, Japan). RT-PCR was conducted with first-strand cDNA as the template and amplified fragments were confirmed using agarose gel electrophoresis. The qRT-PCR was performed with the SYBR Premix Ex Taq II (Takara) on LightCycler480 Real-Time PCR System (Roche, Basel, Switzerland). Primers used for RT-PCR and qRT-PCR were listed in Table S1.

Yeast Two-Hybrid Assays

To test the interaction between KNAT3, KNAT7, NST1 and NST2 proteins, the bait constructs pDEST32-KNAT3 and pDEST32-KNAT7 were generated by LR reaction between pDONR207-KNAT3, pDONR207-KNAT7 plasmids and pDEST32 (Invitrogen). The prey constructs pDEST22-NST1, pDEST22-NST2, pDEST22-KNAT3, and pDEST22-KNAT7 were generated by LR reaction between pDONR207-NST1, pDONR207-NST2, pDONR207-KNAT3, pDONR207-KNAT7 and pDEST22 (Invitrogen). Bait plasmids and prey plasmids or blank pDEST22 were co-transformed into yeast strain AH109. Medium supplemented with SD-Leu-Trp-His and 2.5 mM 3-amino-1,2,4 triazole was used for selection (Tao *et al.*, 2013).

Yeast one-hybrid assay

To test whether KNAT3 and KNAT7 could bind the promoter of *F5H* gene directly, yeast one-hybrid assay was performed. The CDS of *KNAT3* and *KNAT7* genes were amplified by PCR and were inserted to *EcoRI/XhoI* sites of pB42AD vector. The 2171 bp promoter region of *F5H* gene was amplified by PCR and was inserted to *EcoRI/XhoI* sites of pLacZi2μ vector. All the constructions were confirmed by sequencing. The corresponding pB42AD and pLacZi2μ fusion constructions were co-transformed into yeast strain EGY48 containing p8op-LacZ plasmid. The transformants were spread on SD/-His-Trp-Ura dropout plates. After 3 d growth at 30℃, the transformants were copied to SD/-His-Trp-Ura dropout plates containing 80 mg/L X-gal for blue color development. pB42AD-CCA1 and pLacZi2μ-proELF4 combination from (Zhao *et al.*, 2018) was used as positive control.

Firefly split luciferase complementation imaging

Full-length CDS of *KNAT3*, *KNAT7*, *NST1* and *NST2* were amplified from *Arabidopsis* cDNA and then cloned into pDONR207 to generate pENTRY construct. nLUC-KNAT3 or cLUC-KNAT7/NST1/NST2 was generated by LR reactions between pCB1300-nLUC-GW or pCB1300-cLUC-GW and pDONR207-NST1, pDONR207-NST2, pDONR207-KNAT3, pDONR207-KNAT7 (Invitrogen). These plasmids were transformed into *Agrobacterium* strain GV3101. Different combinations of plasmids were co-infiltrated into tobacco leaves. The empty pCB1300-BD-nLUC and pCB1300-cLUC-GW vectors were used as negative controls. After incubation in dark for 24 h and then in light for 72 h, the tobacco leaves were sprayed with 100 mM D-luciferin and kept in dark for 10 min (Han *et al.*, 2019). The fluorescence was detected using a low-light cooled charge-coupled device (CCD) imaging apparatus (NightOWL818 II LB983) with indiGO software.

Transactivation analyses

A 2171bp promoter sequence of *F5H* was amplified from *Arabidopsis* genomic DNA, then recombined into pGreen II 0800-LUC vector, and used as reporter plasmids (Hellens *et al.*, 2005). The coding sequence of *KNAT3*/*KNAT7* was amplified by PCR, inserted into pGreen II 62-SK, and used as an effector plasmid. The effector and reporter were co-transfected into *Arabidopsis* leaf protoplasts (Yoo *et al.*, 2007). After placing them under low-light conditions for 14-16 h, the protoplasts were lysed and the supernatants were assayed for FLUC and

RLUC activities with the Dual-Luciferase Reporter Assay System (Promega, Madison, WI, USA). The LUN/REN ratio indicates transcriptional activity.

Co-immunoprecipitation and immunoblot analyses

Total proteins from *Nicotiana benthamiana* were extracted using IP buffer containing 150 mM NaCl, 50 mM Tris-HCl (pH 7.5), 5 mM EDTA, 10% glycerol, 1% Triton-X 100, 0.2% NP-40, 5mM DTT, and 1 × complete protease inhibitor cocktail. Anti-FLAG M2 Magnetic Beads (Sigma, M8823) was used for immunoprecipitation for HA- and FLAG-tagged proteins. The affinity beads were washed with washing buffer (150 mM NaCl, 50 mM Tris-HCl pH 7.5, 5 mM EDTA, 1% Triton-X 100, 0.2% NP-40, and 1 × complete protease inhibitor cocktail). The protein extraction was incubated with the affinity beads for 4 hours at 4˚C with gentle mixing to capture the proteins. Anti-FLAG (Abmart, M20008) and anti-HA (Abmart, M20003) antibodies from mice were used to detect input proteins; Anti-FLAG (Sigma, F7452) and anti-HA (Sigma, H6908) antibodies from rabbits were used to detect immunoprecipitated proteins. Immunoblots were performed according to the enhanced chemiluminescence western blotting procedure.

RESULTS

Chimeric KNAT3 and KNAT7 repressors induced similar dwarf phenotype

To examine the paradox of KNAT7 negatively and positively regulating secondary cell wall biosynthesis (Zhong *et al.*, 2006; Zhong *et al.*, 2007; Zhong *et al.*, 2008; Li *et al.*, 2011; Li *et al.*, 2012; Zhong and Ye, 2012; He *et al.*, 2018), the KNOX II proteins, including KNAT3, KNAT4, KNAT5 and KNAT7 (Furumizu *et al.*, 2015), were fused with the EAR-motif repressor domain SRDX (Hiratsu *et al.*, 2003; Hiratsu *et al.*, 2004) which converted the individual KNOXII transcription factors into dominant repressors. The chimeric KNOX II repressor cassettes, driven by the cauliflower mosaic virus (CaMV) 35S promoter (p*35S*:KNOX II-SRDX), were expressed in *Arabidopsis* (Fig. S1A). Among all four KNOX II-SRDX transgenic plants, only p*35S*:KNAT3-SRDX and p*35S*:KNAT7-SRDX showed morphological resemblance, displaying a similar dwarf and bush phenotype (Fig. S1B), which suggests a probable functional redundancy of *KNAT3* and *KNAT7* in inflorescence stems.

***KNAT3* and *KNAT7* were co-expressed in the interfascicular fiber and xylem**

To validate the speculated functional redundancy of KNAT3 and KNAT7 in inflorescence stems, we first examined the expression of *KNAT3* and *KNAT7* genes in *Arabidopsis*. The relative transcription levels of *KNAT3* and *KNAT7* in different tissues were detected by qRT-PCR. The results showed that the expression level of *KNAT7* in the stem was much higher than that of *KNAT3*, while compared to *KNAT7*, the expression level of *KNAT3* in the cauline and senescent leaves was higher. (Fig. 1A). To further check expression patterns of *KNAT3* and *KNAT7* in inflorescence stems, the promoter regions of *KNAT3* and *KNAT7* were fused with *GUS* gene, respectively; the resulted vectors p*KNAT3*:GUS and p*KNAT7*:GUS were then transferred into wild-type plants. Despite the p*KNAT3*:GUS showed diffusions in phloem and other cells, the GUS-staining for both p*KNAT3*:GUS and p*KNAT7*:GUS was observed in both xylem and interfascicular fiber cells (Fig. 1D, E). These results confirmed that *KNAT3* and *KNAT7* were co-expressed in the inflorescence stems.

***knat3 knat7* double mutant exhibits severe irregular xylem phenotype**

To further analyze the functional redundancy between KNAT3 and KNAT7, double mutant was obtained by crossing *knat3* (SALK_136464) and *knat7* (SALK_110899) single mutants. RT-PCR analysis showed that transcript fragments of *KNAT3* and *KNAT7* in *knat3* and *knat7* single mutant were not amplified (Fig. 2C), indicating that *KNAT3* and *KNAT7* cannot form an intact mRNA due to the T-DNA insertions, thus these two lines were functional knock-out mutants. Morphologically, *knat3* and *knat7* single mutants shared similar height with wild type (WT), while the *knat3 knat7* double mutant was significantly shorter than WT (Fig. 2D-E).

To elucidate the reason for the difference in height between *knat3* and *knat7* mutant combinations, cross-sections were taken from the base of inflorescence stems of 6-week-old WT, *knat3*, *knat7* and *knat3 knat7* plants. The *knat3*, as did the WT, exhibited normal vessels phenotype, and *knat7* showed slight weak irregular vessels (Fig. 3A-C), whereas severe irregular xylem vessels were clearly observed in the *knat3 knat7* double mutants (Fig. 3D). The thickness of xylem (vessel and xylary) and interfascicular fiber cell walls of WT, *knat3*, *knat7*, and *knat3 knat7* was further measured. Compared with WT, *knat7* had thicker interfascicular fiber cell walls but thinner vessel and xylary cell walls in inflorescence stems(Fig. 3E-G), which are consistent with previous reports (Li *et al.*, 2012; He *et al.*, 2018)**. On the contrary, the cell wall thickness of interfascicular fiber**

became reduced in *knat3*, while all the vessel, xylary and interfascicular fiber cell wall thicknesses were significantly thinner in *knat3knat7* double mutant. These results indicate that KNAT3 and KNAT7 have functional redundancy in regulating at least the xylem vessel and xylary secondary cell wall development .

The complementation was performed to investigate whether the phenotype of *knat3 knat7* double mutant was indeed caused by knockout of the corresponding genes. The full-length coding sequences of *KNAT3* and *KNAT7* were fused with CaMV35S promoter and transferred to *knat3 knat7* mutant. The transgenic lines fully rescued the dwarfism and **the irregular xylem** phenotype **of the mutant (Fig. 2F and Fig. 3H). These results confirm that the phenotype of *knat3 knat7* mutant is indeed caused by the loss of function of *KNAT3* and *KNAT7*.**

KNAT3 and KNAT7 synergistically regulate syringyl lignin biosynthesis

Mäule staining was performed on stem cross-section of p*35S*:KNAT3-SRDX and p*35S*:KNAT7-SRDX repressor transgenic plants to examine chemical changes in cell wall composition of *knat3* and *knat7* mutants (Fig. S2). The wild-type xylem was stained bright-red, the p*35S*:KNAT7-SRDX xylem was stained weak brown-red, whereas the p*35S*:KNAT3-SRDX xylem was stained yellow-brown (Fig. S2). These results indicate that the synthesis of S-lignin might be significantly inhibited in KNAT3 repressor transgenic plants.

To verify whether the lignin defect in the chimeric KNAT3 and KNAT7 repressors corresponds to *knat3 knat7* mutation, lignin content in *KNAT3* and *KNAT7* mutants was further determined. The results showed that acid-soluble lignin in the *knat3* and *knat3 knat7* mutants was significantly reduced compared to the WT. However, no significant changes were found in the acid-insoluble lignin and total amount of lignin in the *knat3*, *knat7* and *knat3 knat7* mutants compared to WT (Fig. 4A-4C). Furthermore, Mäule staining showed that the stem section of the *knat3 knat7* mutant stained yellow-brown (Fig. 4D-4G), which is consistent with the observation in domain repressor plants. Meanwhile，the stem cross-sections of *KNAT3* and *KNAT7* complementation plants in *knat3 knat7* double mutant rescued the color changes from yellow-brown to bright-red (Fig. S3). These results indicate a decrease in S-lignin in the *knat3 knat7* double mutant.

To determine the amount of S-lignin reduction, GC-MS was used to detect the content of S- and G-lignin monomers (Table 1). G-lignin was significantly reduced in *knat3*, while

significantly increased in *knat7* and *knat3 knat7*. Due to significant downregulation of both G-lignin and S-lignin in *knat3*, S/G ratio showed no change whereas the S/G ratio in *knat7* decreased because of an increase in G-lignin and a slight decrease in S-lignin (Table 1). Furthermore, S-lignin content further reduced by about 80% in *knat3 knat7* double mutant compared to WT, which resulted in an 84% reduction of S/G ratio in *knat3 knat7*. Additional 2D Heteronuclear Single Quantum Coherence (HSQC) spectra of WT and *knat3 knat7* cell wall samples were collected to figure out the differences of lignin (Fig. 4H). The correlations in the HSQC spectra of whole cell wall preparations were assigned by comparison with the published data (Kim and Ralph, 2010; Mansfield *et al.*, 2012). As showed in Figure 4H, both G- and S-lignin signals were detected in the WT cell walls, although the amount of S units was much lower than that of G units, which is consistent with thioacidolysis analysis (Table 1). However, in HSQC spectra of *knat3 knat7*, the correlations of S unit ($S_{2/6}$) was completely absent, while the correlations of G unit and H unit lignin subunits were much stronger than those of WT, which indicates a much higher amount of G lignin in *knat3 knat7*. Overall, 2D HSQC confirms an increase in G-lignin and a decrease in S lignin in *knat3 knat7* mutant.

The key S-lignin biosynthetic gene *FERULATE-5-HYDROXYLASE* (*F5H*) was down-regulated in *knat3 knat7* mutant

To further explain the decrease of S-lignin in the *knat3 knat7* mutant, the main stem of 6-week-old WT and *knat3 knat7* mutant were collected for RNA sequencing. Data analysis showed that the differentially expressed genes were significantly enriched in the phenylalanine metabolic pathway (Fig. S4), which is consistent with the phenotype of *knat3 knat7* mutant showing a significant decrease in the proportion of lignin S/G. Interestingly, the expression profiles of lignin metabolic pathway genes *CCR*, *COMT*, *CCoAOMT*, and *CAD* were up-regulated (Fig. 5A) and expression levels of *4CL1* and *F5H* were down-regulated. The increasing G-lignin content in *knat3 knat7* could be due to the activation of parts of lignin pathway genes, such as G-lignin related *CCoAOMT*. Because *F5H* is a key enzyme for the synthesis of S-lignin (Franke *et al.*, 2000; Garcia *et al.*, 2014), the reduced *F5H* expression might attribute to the decrease of S-lignin content in the *knat3 knat7* mutant . Furthermore, the RNA-seq results were verified by qRT-PCR analysis of lignin biosynthetic genes in WT and *knat3 knat7* mutants, in which *F5H* expression was reduced by 77% (Fig. 5B).

KNAT3 plays main effect on regulating the expression of *F5H* gene

Because the significant decrease of S-lignin in *knat3 knat7* might be caused by the down-regulation of *F5H* expression, we explored whether *KNAT3* and *KNAT7* can regulate the expression of the *F5H* gene. 2171 bp upstream region of *F5H* gene was cloned and constructed into a reporter vector harboring luciferase (LUC) gene, the p*35S*:KNAT3 and p*35S*:KNAT7 were constructed as effectors (Fig. 6A), and transiently transformed into *Arabidopsis* protoplast cells. The results showed that both KNAT3 and KNAT7 can activate the luciferase (LUC) expression, KNAT3 had higher activity than KNAT7, and KNAT3+KNAT7 combination showed the highest activation (Fig. 6B). These results indicate that KNAT3 and KNAT7 can work on *F5H* promoter to regulate LUC expression.

In order to detect whether KNAT3 and KNAT7 can directly or indirectly activate *F5H* genes, yeast one-hybrid system was used to check the binding effects. Unexpectedly, neither KNAT3 nor KNAT7 bound directly to the *F5H* promoter region (Fig. 6C). Therefore, we hypothesize that KNAT3 and KNAT7 might activate other genes or form a protein complex to regulate the expression of *F5H*. Up until now there are no proteins reported to directly regulate *F5H* in *Arabidopsis*, so we speculate that the regulation of *F5H* may be accomplished by a certain bigger complex.

KNOXs, as members of TALE homeodomain superfamily (Hake *et al.*, 2004; Hay and Tsiantis, 2010), have potential to form homo- or hetero- dimers. We did find that KNAT3 and KNAT7 can form homo-dimer and hetero-dimer in yeast two-hybrid assay (Fig. 6D, 6E), as reported by Hackbusch et al., (2005). Split luciferase complementation experiments verified that KNAT3 and KNAT7 form dimers in *planta* as well (Fig. 6F). Therefore, when introduced KNAT3 and KNAT7 simultaneously into the *Arabidopsis* protoplast cells, we found that the mixture of KNAT3 and KNAT7 showed a stronger activation effect than KNAT3 alone (Fig. 6B), suggesting that heterodimer might have better effect than homodimer.

KNAT3 but not KNAT7 interacts with NST1 and NST2 to regulate the expression of *F5H* gene

Since neither KNAT3 nor KNAT7 directly binds to the *F5H* promoter but they showed weak activation of *F5H* expression, we deduced that some proteins/factors in the regulation system were missed. Hence, we used KNAT3 as a bait protein to screen an *Arabidopsis* transcription factor library by yeast two-hybrid screening (Mitsuda *et al.*, 2010). *NST1* and *NST2* were identified in screening, which have been regarded as the top-level switches to regulate secondary cell wall formation (Mitsuda *et al.*, 2005; 2007; Zhong *et al.*, 2010; Zhou *et al.*, 2014; Zhong and Ye, 2015). We further verified the interactions between KNAT3/7 and NST1, NST2, SND1 (also named as NST3) by yeast two-hybrid, split-luciferase complementation and co-immunoprecipitation and immunoblot analyses (Fig. 7A-7E). The results showed that only KNAT3, but not KNAT7, interacted with NST1 and NST2. Neither KNAT3 nor KNAT7 can interact with SND1 (Fig. 7A-7E).

Furthermore, we investigated whether the heterologous complex formed by KNAT3 and NST1/NST2 activates *F5H* expression. We performed transcriptional activation experiment in *Arabidopsis* protoplasts. The results revealed that NST1 and NST2 alone could weakly activate the *F5H* promoter, and no further activation was gained after KNAT3 was added (Fig. 7F). This indicates that some factors in regulating *F5H* expression might still be missing and are required for further exploration.

DISCUSSION

There are four members of *Arabidopsis KNOX* class II genes, among which *KNAT3*, *KNAT4* and *KNAT5* play a functionally redundant role in regulating leaf morphology, and the serrated leaf phenotypes of *knat3*, *knat3 knat5*, and *knat3 knat4 knat5* increase gradually (Furumizu *et al.*, 2015). However, the effects of *KNAT3*, *KNAT4* and *KNAT5* on secondary wall formation have not been reported. *KNAT7*, also called *IRX11*, has been reported to link with vessel cell development as its mutant showing inwardly collapsed vessel cells thus forming irregular xylem (Brown *et al.*, 2005). Some reports revealed that KNAT7 acts as a transcriptional repressor to inhibit the secondary cell wall deposition (Li *et al.*, 2011; Li *et al.*, 2012), but *knat7* mutant showed thinner vessel cell despite thicker interfascicular fiber cell (Li *et al.*, 2012). KNAT7 can also act as a transcriptional activator to activate the expression of xylan synthesis genes (He *et al.*, 2018). To better explain this contradiction, we further combined

other KNOX II members with KNAT7 in the study. We found that KNAT3 and KNAT7 had obvious functional redundancy in regulating the synthesis of *Arabidopsis* secondary cell wall. Coincidentally, Wang *et al.*, 2019 recently reported *KNAT3* and *KNAT7* work cooperatively to influence secondary cell wall deposition. Their work was mainly focused on the functions of KNAT3 and KNAT7 on secondary cell wall synthesis, including hemicellulose and lignin synthesis. They introduced the phenotype and chemical analysis results and their conclusions are in close agreement with ours. In present study, we focused on lignin, especially S- lignin subunit, and we explained the reason why the S-subunit lignin decreases in mutant by protein interaction and pathway analysis.

Dominant repressor plants (p*35S*:KNAT3-SRDX and p*35S*:KNAT7-SRDX) displayed severe defects in stem development and both showed similar dwarf phenotypes (Fig. S1) indicating that these genes exhibit functional redundancy. The expression patterns demonstrated that *KNAT3* and *KNAT7* were co-expressed in secondary xylem and interfascicular fiber tissues (Fig. 1). The loss-of-function of *knat3 knat7* double mutant showed significantly reduced height at 6-week-old (Fig. 2D, E), which is consistent with *KNAT3* and *KNAT7* dominant repressor plants. In addition to irregular xylem, the *knat7* mutant showed thicker interfascicular fiber wall, thinner xylem vessel wall and increased lignin content (Li *et al.*, 2011; He *et al.*, 2018). Literature reports that KNAT7 interacts with MYB75, BLH6 and OFP4, forming a complex to inhibit the secondary cell wall formation (Hackbusch *et al.*, 2005; Bhargava *et al.*, 2010; Li *et al.*, 2011; Liu *et al.*, 2014), which indicates that KNAT7 has complicated and spatiotemporally differentiated functions based on specific cell type, tissue and interacting regulators. *knat3* differs from *knat7* in that *knat3* has no irregular xylem phenotype but thinner secondary cell wall in interfascicular fiber cell. However, *knat3 knat7* has an enhanced *irx* phenotype (Fig. 3) and significantly reduced cell wall thickness in vessel, xylary and interfascicular fiber as compared to *knat7*. This phenotype indicated that KNAT3, as a homolog of KNAT7, has functional redundancy in the development of secondary cell wall, and KNAT3 can be a transcriptional activator of secondary wall thickening. We found KNAT3 and KNAT7 proteins can form heterodimers in the yeast two-hybrid assay and only KNAT3 interacts with NST1 and NST2, the two mast regulators involved in regulation of secondary cell wall thickening (Mitsuda *et al.*, 2005; Zhong and Ye, 2015). Based on these results, we proposed a working model of KNAT3 and KNAT7 as shown in figure 8. The KNAT3 interacts with NST1/2, the positive regulators of secondary cell wall, but KNAT7 interacts with MYB75/ BLH6/ OFP4,— the negative regulators of secondary cell wall.

Interestingly, secondary cell wall in interfascicular fibers thickness was lost in *nst1 nst3* double mutant (Zhong *et al.*, 2007; Zhong and Ye, 2015) meaning that NST1 can specifically function in this region. Thus, we speculate that, in *knat7* mutant, KNAT3 and NST1 complex stimulate the downstream genes to promote cell wall synthesis in interfascicular fiber and produce thicker interfascicular fiber wall. At the same time, *NST1* is a fiber-specific transcription factor and KNAT3 might interact with NST1. S lignin is predominantly deposited in fiber regions, so *knat3* mutant showed lower fiber cell wall thickness (Figure 3 F and G), and lower S-lignin (Table 1).

In dicots, lignin is mainly composed of S- and G-lignin subunits and a very low concentration of H-lignin (Vogel, 2008). Acid-soluble lignin was preferentially derived from the condensed syringyl lignin while the guaiacyl lignin was insoluble in 72% sulfuric acid (Yue *et al.*, 2012) .It is possible that acid-soluble lignin has relative high S-lignin content, and acid-insoluble lignin contains high G-lignin content (Fig. 4A). Thus, the lower acid-insoluble lignin might be resulted from the lower content of S-lignin in the *knat3* and *knat3 knat7*, as compared with *knat7* and WT (Fig. 4A and Table 1). Some reports suggest that KNAT7 is a negative regulator of lignin biosynthesis and the loss-function mutant of *knat7* had increased lignin content (Brown *et al.*, 2005; Li *et al.*, 2011). Our determination of lignin content evidenced that the increase of total lignin content in *knat7* was due to a large increase of G-lignin with concomitant slight decrease of S-lignin. The contents of G, S and total lignin in *knat3* were significantly reduced, but the lignin S/G ratio remained unchanged, indicating KNAT3 positively regulates lignin biosynthesis. Although the total lignin in the *knat3 knat7* remained unchanged, the S-lignin was greatly reduced and the G-lignin was increased, eventually resulting in an 84% reduction of the S/G ratio (Fig. 4 and Table 1). Therefore, we believe that KNAT3 synergizes with KNAT7 in lignin synthesis, and KNAT3 plays a dominant role in controlling S-lignin synthesis.

In lignin synthesis pathway, F5H is a key enzyme responsible for hydroxylation of G-lignin monomer to form S-lignin (Humphreys *et al.*, 1999; Osakabe *et al.*, 1999; Franke *et al.*, 2000; Garcia *et al.*, 2014). Our transcriptomic data of *knat3 knat7* indicated that the differentially expressed genes were significantly enriched in the phenylalanine metabolic pathway (Fig. S4) and most of the gene expression was up-regulated, while the expression levels of *4CL* and *F5H* were down-regulated (Fig. 5). Therefore, the down-regulation of *F5H* could contribute to the increased G-lignin in *knat7* mutant with the unchanged total lignin contents in most mutants. This is also a good explanation for the increase in G-lignin content and the large

reduction of S-lignin in *knat3 knat7*. We also checked the profiles of all MYB transcription factors in our transcriptome data. We found that MYB20, MYB69 and MYB86 were down-regulated, however, both *MYB46* / *MYB83*, regarded as activators of secondary wall biosynthesis and *MYB75*/*MYB4* / *MYB7*, regarded as repressors of secondary wall biosynthesis were up-regulated (supplemental table 2) (McCarthy *et al.*, 2009; Bhargava *et al.*, 2010b; Ko *et al.*, 2014; Wang *et al.*, 2019). Thus, KNAT3 and KNAT7 might have a complicated regulatory network or feedback network. Because the *myb103* mutant can also decrease *F5H* gene expression level (Ohman *et al.*, 2013), it is unclear whether MYB103 works at upstream or downstream of KNAT3/KNAT7 on regulating *F5H* gene expression. According to our transcriptome and qPCR analysis, the *MYB103* expression level showed no obvious difference in *knat3 knat7* double mutant, compared to the WT (Table S2 and Fig S5 A and B); and the expression levels of *KNAT3* and *KNAT7* increased in *myb103* mutant (Fig S5 B). The increased *KNAT7* expression is especially obvious. The cause of increased *KNAT3/7* expression might be due to compensation. All results indicate that MYB103 and KNAT3/KNAT7 might function in independent pathway to regulate *F5H* expression.

Transcriptional activation experiments in *Arabidopsis* protoplasts revealed that both KNAT3 and KNAT7 weakly activated the *F5H* promoter, suggesting that KNAT3 and KNAT7 indirectly regulate *F5H* (Fig. 6). It is known that MYB58 and MYB63 directly activate the expression of lignin-synthetic genes by binding to the AC element or degenerated AC element of the promoter regions of those genes (Zhou *et al.*, 2009; Zhao and Dixon, 2011). However, there is no AC element in the *F5H* promoter region, except that NST1 and SND1 were reported to bind directly to the F5H promoter region to activate *F5H* expression in *Medicago truncatula* (Zhao *et al.*, 2010). *Arabidopsis* SND1 cannot directly activate *F5H* expression (Ohman *et al.*, 2013). Our yeast one-hybrid experiments showed that neither KNAT3 nor KNAT7 could directly bind to the promoter of *F5H*. Only KNAT3, not KNAT7, interacts with the secondary cell wall top regulatory factors NST1/NST2. Although NST1 and NST2 can weakly activate *F5H* expression, it may be still missing some effectors in the regulatory cascade or complex (Fig. 7). *F5H* regulation mechanism remains to be further explored.

As we know, fibers are enriched in S-lignin, whereas guaiacyl-enriched lignin is mainly deposited in vessels (Fergus and Goring, 1970a, 1970b; Msha and Goring, 1975; Saka and Goring, 1985). Furthermore, the deposition of S-lignin precedes that of G-lignin in interfascular fiber elements (Terashima et al., 1986; Saka and Goring, 1988). NST1 and

NST2 belong to fiber-specific transcription factors, which interact with KNAT3, could be the reason for S-lignin biosynthesis via activating F5H in the fiber. Although *knat3 knat7* mutant has collapsed vessels as the *knat7* mutant, both mutants contain increased G-lignin content, and the expression of G-lignin pathway genes, such as CCoAOMT is up-regulated as well. To investigate the cause of increase in G-lignin, the expression of VASCULAR-RELATED NAC-DOMAIN 6 (VND6) and 7 (VND7), which work as master regulators of metaxylem and protoxylem vessel cell fates, respectively (kubo et al., 2005; Ohashi-Ito et al., 2010), was examined in the transcriptome analysis. The result showed that the expression of VND6 and VND7 only slightly decreased in *knat3 knat7* mutant in comparison with WT (Fig S5A). Additionally, we did not detect the interactions between KNAT7 and VND6/7 by yeast-two hybrid (Data not shown). Thus, we deduce that the increasing G-lignin content in *knat3 knat7* might be due to the increase of some G-lignin biosynthetic related genes and down-regulation of *F5H*.

This study demonstrates that KNAT3 and KNAT7 play a synergistic role in regulating the growth and development of *Arabidopsis* secondary cell wall. The *KNAT3* mutant enhances the phenotype of *knat7* in the secondary cell wall of xylem vessels (Fig. 3, 4). In addition, KNAT3 interacts with NST1/NST2 to promote *F5H* to regulate the synthesis of S-lignin. In the synthesis of secondary cell wall including lignin, interactions such as KNAT7 and BLH6/MYB75/OFP4 may function as transcriptional repressors. On the other hand, KNAT3 synergizing with KNAT7 functions positively for the synthesis of S-lignin (Fig. 8). This study complements the transcriptional regulatory network of secondary cell walls and clarifies the regulation of S-lignin by KNAT3 and KNAT7.

DATA STATEMENT

All relevant data can be found within the manuscript and its supporting materials.

ACKNOWLEDGEMENTS

We thank the Arabidopsis Biological Resource Center for seeds of the T-DNA insertion mutant. Financial support for this work was obtained the National Natural Science Foundation of China (Grant Numbers 31870653, 31670670, 31811530009).

CONFLICT OF INTEREST

The authors have no conflicts of interest to declare.

AUTHOR CONTRIBUTION

AM Wu, and W Qin designed the study and wrote the manuscript. W Qin, Q Yin, X zhao, J Chen, F Yue, J he, L Yang, L liu, performed the experiments, F Lu Wang, N Mitsuda, M Ohme-Takagi contributed to the techniques help and analyzed the data.

REFERENCES

Bhargava A, Mansfield SD, Hall HC, Douglas CJ, Ellis BE. 2010a. MYB75 functions in regulation of secondary cell wall formation in the Arabidopsis inflorescence stem. Plant Physiology **154**, 1428-1438.

Bhargava A, Mansfield SD, Hall HC, Douglas CJ, Ellis BE. 2010b. MYB75 functions in regulation of secondary cell wall formation in the Arabidopsis inflorescence stem. Plant Physiology **154,** 1428-1438.

Boerjan W, Ralph J, Baucher M. 2003. Lignin biosynthesis. Annual Review of Plant Biology **54,** 519-546.

Bonawitz ND, Chapple C. 2010. The genetics of lignin biosynthesis: Connecting genotype to phenotype. Annual Review of Genetics **44,** 337-363.

Brown DM, Zeef LA, Ellis J, Goodacre R, Turner SR. 2005. Identification of novel genes in Arabidopsis involved in secondary cell wall formation using expression profiling and reverse genetics. Plant Cell **17,** 2281-2295.

Clough SJ, Bent AF. 1998. Floral dip: A simplified method for Agrobacterium-mediated transformation of Arabidopsis thaliana. Plant Journal **16,** 735-743.

Cosgrove DJ, Jarvis MC. 2012. Comparative structure and biomechanics of plant primary and secondary cell walls. Frontiers in Plant Science **3,** 204.

Fergus, B.J., and Goring, D.A.I. 1970a. The location of guaiacyl and syringyl lignins in birch xylem tissue. Holzforschung **24**.

Fergus, B.J., and Goring, D.A.I. 1970b. The distribution of lignin in birch wood as determined by ultraviolet microscopy. Holzforschung **24,** 118–124.

Franke R, McMichael CM, Meyer K, Shirley AM, Cusumano JC, Chapple C. 2000. Modified lignin in tobacco and poplar plants over-expressing the Arabidopsis gene encoding ferulate 5-hydroxylase. Plant Journal **22,** 223-234.

Furumizu C, Alvarez JP, Sakakibara K, Bowman JL. 2015. Antagonistic roles for KNOX1 and KNOX2 genes in patterning the land plant body plan following an ancient gene duplication. PLoS Genetics **11,** e1004980.

Garcia JR, Anderson N, Le-Feuvre R, Iturra C, Elissetche J, Chapple C, Valenzuela S. 2014. Rescue of syringyl lignin and sinapate ester biosynthesis in Arabidopsis thaliana by a coniferaldehyde 5-hydroxylase from Eucalyptus globulus. Plant Cell Reports **33,** 1263-1274.

Goicoechea M, Lacombe E, Legay S, *et al*. 2005. EgMYB2, a new transcriptional activator from Eucalyptus xylem, regulates secondary cell wall formation and lignin biosynthesis. Plant Journal **43,** 553-567.

Hackbusch J, Richter K, Muller J, Salamini F, Uhrig JF. 2005. A central role of Arabidopsis thaliana ovate family proteins in networking and subcellular localization of 3-aa loop extension homeodomain proteins. Proceedings of the National Academy of Sciences of the United States of America **102,** 4908-4912.

Hake S, Smith HM, Holtan H, Magnani E, Mele G, Ramirez J. 2004. The role of knox genes in plant development. Annual Review of Cell and Developmental Biology **20,** 125-151.

Han X, Yu H, Yuan R, Yang Y, An F, Qin G. 2019. Arabidopsis transcription factor TCP5 controls plant thermomorphogenesis by positively regulating PIF4 activity. iScience **15,** 611-622.

Hay A, Tsiantis M. 2010. KNOX genes: Versatile regulators of plant development and diversity. Development **137,** 3153-3165.

He JB, Zhao XH, Du PZ, Zeng W, Beahan CT, Wang YQ, Li HL, Bacic A, Wu AM. 2018. KNAT7 positively regulates xylan biosynthesis by directly activating IRX9 expression in Arabidopsis. Journal of Integrative Plant Biology **60,** 514-528.

Hellens RP, Allan AC, Friel EN, Bolitho K, Grafton K, Templeton MD, Karunairetnam S, Gleave AP, Laing WA. 2005. Transient expression vectors for functional genomics, quantification of promoter activity and RNA silencing in plants. Plant Methods **1,** 13.

Hiratsu K, Matsui K, Koyama T, Ohme-Takagi M. 2003. Dominant repression of target genes by chimeric repressors that include the EAR motif, a repression domain, in Arabidopsis. Plant Journal **34,** 733-739.

Hiratsu K, Mitsuda N, Matsui K, Ohme-Takagi M. 2004. Identification of the minimal repression domain of SUPERMAN shows that the DLELRL hexapeptide is both necessary and sufficient for repression of transcription in Arabidopsis. Biochemical and Biophysical Research Communications **321,** 172-178.

Humphreys JM, Hemm MR, Chapple C. 1999. New routes for lignin biosynthesis defined by biochemical characterization of recombinant ferulate 5-hydroxylase, a multifunctional cytochrome P450-dependent monooxygenase. Proceedings of the National Academy of Sciences of the United States of America **96,** 10045-10050.

Jefferson RA, Kavanagh TA, Bevan MW. 1987. GUS fusions: Beta-glucuronidase as a sensitive and versatile gene fusion marker in higher plants. EMBO Journal **6,** 3901-3907.

Kerstetter R, Vollbrecht E, Lowe B, Veit B, Yamaguchi J, Hake S. 1994. Sequence analysis and expression patterns divide the maize knotted1-like homeobox genes into two classes. Plant Cell **6,** 1877-1887.

Kim H, Ralph J. 2010. Solution-state 2D NMR of ball-milled plant cell wall gels in DMSO-d(6)/pyridine-d(5). Organic & Biomolecular Chemistry **8,** 576-591.

Ko JH, Jeon HW, Kim WC, Kim JY, Han KH. 2014. The MYB46/MYB83-mediated transcriptional regulatory programme is a gatekeeper of secondary wall biosynthesis. Annals of Botany **114,** 1099-1107.

Kubo M., Udagawa M., Nishikubo N., Horiguchi G., Yamaguchi M., Ito J., Mimura T., Fukuda H., Demura T. 2005. Transcription switches for protoxylem and metaxylem vessel formation. Genes Dev **19,** 1855–1860.

Lacombe E, Van Doorsselaere J, Boerjan W, Boudet AM, Grima-Pettenati J. 2000. Characterization of cis-elements required for vascular expression of the cinnamoyl CoA reductase gene and for protein-DNA complex formation. Plant Journal **23,** 663-676.

Li E, Bhargava A, Qiang W, Friedmann MC, Forneris N, Savidge RA, Johnson LA, Mansfield SD, Ellis BE, Douglas CJ. 2012. The Class II KNOX gene KNAT7 negatively regulates secondary wall formation in Arabidopsis and is functionally conserved in Populus. New Phytologist **194,** 102-115.

Li E, Wang S, Liu Y, Chen JG, Douglas CJ. 2011. OVATE FAMILY PROTEIN4 (OFP4) interaction with KNAT7 regulates secondary cell wall formation in Arabidopsis thaliana. Plant Journal **67,** 328-341.

Liu Y, You S, Taylor-Teeples M, Li WL, Schuetz M, Brady SM, Douglas CJ. 2014. BEL1-LIKE HOMEODOMAIN6 and KNOTTED ARABIDOPSIS THALIANA7 interact and regulate secondary cell wall formation via repression of REVOLUTA. Plant Cell **26,** 4843-4861.

Mansfield SD, Kim H, Lu F, Ralph J. 2012. Whole plant cell wall characterization using solution-state 2D NMR. Nature Protocols **7,** 1579-1589.

McCarthy RL, Zhong R, Ye ZH. 2009. MYB83 is a direct target of SND1 and acts redundantly with MYB46 in the regulation of secondary cell wall biosynthesis in Arabidopsis. Plant And Cell Physiology **50,** 1950-1964.

Mitsuda N, Hiratsu K, Todaka D, Nakashima K, Yamaguchi-Shinozaki K, Ohme-Takagi M. 2006. Efficient production of male and female sterile plants by expression of a chimeric repressor in Arabidopsis and rice. Plant Biotechnology Journal **4,** 325-332.

Mitsuda N, Ikeda M, Takada S, Takiguchi Y, Kondou Y, Yoshizumi T, Fujita M, Shinozaki K, Matsui M, Ohme-Takagi M. 2010. Efficient yeast one-/two-hybrid screening using a library composed only of transcription factors in Arabidopsis thaliana. Plant And Cell Physiology **51,** 2145-2151.

Mitsuda N, Seki M, Shinozaki K, Ohme-Takagi M. 2005. The NAC transcription factors NST1 and NST2 of Arabidopsis regulate secondary wall thickenings and are required for anther dehiscence. Plant Cell **17,** 2993-3006.

Mukherjee K, Brocchieri L, Burglin TR. 2009. A comprehensive classification and evolutionary analysis of plant homeobox genes. Molecular Biology And Evolution **26,** 2775-2794.

Musha, Y., and Goring, D.A.I. 1975. Distribution of syringyl and guaiacyl moieties in hardwoods as indicated by ultraviolet microscopy. Wood Science And Technology. **9,** 45–58.

Nakagawa T, Suzuki T, Murata S, *et al.* 2007. Improved Gateway binary vectors: High-performance vectors for creation of fusion constructs in transgenic analysis of plants. Bioscience Biotechnology And Biochemistry **71,** 2095-2100.

Ohman D, Demedts B, Kumar M, Gerber L, Gorzsas A, Goeminne G, Hedenstrom M, Ellis B, Boerjan W, Sundberg B. 2013. MYB103 is required for FERULATE-5-HYDROXYLASE expression and syringyl lignin biosynthesis in Arabidopsis stems. Plant Journal **73,** 63-76.

Ohashi-Ito K, Oda Y, Fukuda H. 2010. Arabidopsis VASCULAR-RELATED NAC-DOMAIN6 Directly Regulates the Genes That Govern Programmed Cell Death and Secondary Wall Formation during Xylem Differentiation. Plant Cell. **22,** 3461-3473.

Osakabe K, Tsao CC, Li L, Popko JL, Umezawa T, Carraway DT, Smeltzer RH, Joshi CP, Chiang VL. 1999. Coniferyl aldehyde 5-hydroxylation and methylation

direct syringyl lignin biosynthesis in angiosperms. Proceedings of the National Academy of Sciences of the United States of America **96,** 8955-8960.

Patzlaff A, McInnis S, Courtenay A, *et al.* 2003. Characterisation of a pine MYB that regulates lignification. Plant Journal **36,** 743-754.

Pradhan MP, Loque D. 2014. Histochemical staining of Arabidopsis thaliana secondary cell wall elements. Journal Visualized Experiments.

Saka, S., and Goring, D.A.I. 1985. Localization of lignin in wood cell walls. In Biosynthesis and Biodegradation of Wood Components, T. Higuchi, ed (New York: Academic Press), pp. 141–160.

Tao Q, Guo D, Wei B, *et al.* 2013. The TIE1 transcriptional repressor links TCP transcription factors with TOPLESS/TOPLESS-RELATED corepressors and modulates leaf development in Arabidopsis. Plant Cell **25,** 421-437.

Vanholme R, Cesarino I, Rataj K, *et al.* 2013. Caffeoyl shikimate esterase (CSE) is an enzyme in the lignin biosynthetic pathway in Arabidopsis. *Science* **341,** 1103-1106.

Vogel J. 2008. Unique aspects of the grass cell wall. Current Opinion in Plant Biology **11,** 301-307.

Wang KL, Wang B, Hu R, Zhao X, Li H, Zhou G, Song L, Wu AM. 2019. Characterization of hemicelluloses in Phyllostachys edulis (moso bamboo) culm during xylogenesis. Carbohydrate Polymers **221,** 127-136.

Wang S, Yamaguchi M, Grienenberger E, Martone PT, Samuels AL, Mansfield SD. 2019. The Class II KNOX genes KNAT3 and KNAT7 work cooperatively to influence secondary cell wall deposition and provide mechanical support to Arabidopsis stems. Plant Journal doi: 10.1111/tpj.14541.

Wang XC, Wu J, Guan ML, Zhao CH, Geng P, Zhao Q. 2019. Arabidopsis MYB4 plays dual roles in flavonoid biosynthesis. Plant Journal doi: 10.1111/tpj.14570.

Wu AM, Rihouey C, Seveno M, Hornblad E, Singh SK, Matsunaga T, Ishii T, Lerouge P, Marchant A. 2009. The Arabidopsis IRX10 and IRX10-LIKE glycosyltransferases are critical for glucuronoxylan biosynthesis during secondary cell wall formation. Plant Journal **57,** 718-731.

Yoo SD, Cho YH, Sheen J. 2007. Arabidopsis mesophyll protoplasts: A versatile cell system for transient gene expression analysis. Nature Protocols **2,** 1565-1572.

Yue F, Lu F, Sun RC, Ralph J. 2012. Syntheses of lignin-derived thioacidolysis monomers and their uses as quantitation standards. Journal of Agricultural and Food Chemistry **60,** 922-928.

Zhao Q, Dixon RA. 2011. Transcriptional networks for lignin biosynthesis: More complex than we thought? Trends in Plant Science **16,** 227-233.

Zhao Q, Wang H, Yin Y, Xu Y, Chen F, Dixon RA. 2010. Syringyl lignin biosynthesis is directly regulated by a secondary cell wall master switch. Proceedings of the National Academy of Sciences of the United States of America **107,** 14496-14501.

Zhao X, Jiang Y, Li J, Huq E, Chen ZJ, Xu D, Deng XW. 2018. COP1 SUPPRESSOR 4 promotes seedling photomorphogenesis by repressing CCA1 and PIF4 expression in Arabidopsis. Proceedings of the National Academy of Sciences of the United States of America **115,** 11631-11636.

Zhong R, Demura T, Ye ZH. 2006. SND1, a NAC domain transcription factor, is a key regulator of secondary wall synthesis in fibers of Arabidopsis. Plant Cell **18,** 3158-3170.

Zhong R, Lee C, Ye ZH. 2010. Global analysis of direct targets of secondary wall NAC master switches in Arabidopsis. Molecular Plant **3,** 1087-1103.

Zhong R, Lee C, Zhou J, McCarthy RL, Ye ZH. 2008. A battery of transcription factors involved in the regulation of secondary cell wall biosynthesis in Arabidopsis. Plant Cell **20,** 2763-2782.

Zhong R, Richardson EA, Ye ZH. 2007. Two NAC domain transcription factors, SND1 and NST1, function redundantly in regulation of secondary wall synthesis in fibers of Arabidopsis. Planta **225,** 1603-1611.

Zhong R, Ye ZH. 2012. MYB46 and MYB83 bind to the SMRE sites and directly activate a suite of transcription factors and secondary wall biosynthetic genes. Plant And Cell Physiology **53,** 368-380.

Zhong R, Ye ZH. 2015. The Arabidopsis NAC transcription factor NST2 functions together with SND1 and NST1 to regulate secondary wall biosynthesis in fibers of inflorescence stems. Plant Signaling & Behavior **10,** e989746.

Zhou J, Lee C, Zhong R, Ye ZH. 2009. MYB58 and MYB63 are transcriptional activators of the lignin biosynthetic pathway during secondary cell wall formation in Arabidopsis. Plant Cell **21,** 248-266.

Zhou J, Zhong R, Ye ZH. 2014. Arabidopsis NAC domain proteins, VND1 to VND5, are transcriptional regulators of secondary wall biosynthesis in vessels. PLoS One **9,** e105726.

TABLE:

Table 1. Determination of Lignin monomer .

Sample	G(μmol/g)	S (μmol/g)	S+G (μmol/g)	S/G
knat3	24.6±0.36***	10.4±0.56***	35±0.78***	0.42±0.021
knat7	49.3±0.45***	14.2±0.79*	63.48±1.24***	0.29±0.014***
knat3 knat7	46.8±1.04***	3.2±0.26***	50±0.92	0.07±0.006***
WT	36.7±0.81	16.2±0.70	52.9±1.37	0.44±0.015

The 8-week-old main stem of Arabidopsis thaliana was selected to determine lignin monomer contents. G: Guaiacyl lignin S: Syringyl lignin. Significant differences with WT were marked as *, * indicates $P < 0.05$, *** indicates $P < 0.001$ based on student's *t*-test. Data is mean ± SD, including three replicates.

FIGURE LEGENDS

Figure 1： The expression pattern of *KNAT3* and *KNAT7*.

(A) Relative expression levels of *KNAT3* and *KNAT7* at different tissues in 6-week-old *Arabidopsis* measured by qRT-PCR. Column height indicates the mean value ± standard deviation of the sample expression, the number n=4, The expression level of *KNAT3* in the WT was "1", *ACT8* was used as an internal reference. (B) and (C) are schematic diagrams of the p*KNAT3*:GUS and p*KNAT7*:GUS cassette, respectively. Red indicates the promoter, green indicates the GUS gene, and blue indicates the terminator. The GUS staining images were shown in p*KNAT3*:GUS (D) and p*KNAT7*:GUS (E), which samples fetched from the base of the 6-week-old stem. If, interfascicular fibers; x, xylem bar=20 μm.

Figure 2. The morphology of *knat3 knat7* double mutant.

Schematic diagrams represent the T-DNA insertion positions of *knat3* (A) and *knat7* (B). The boxes and lines were instead of exons and introns, respectively, and the triangle indicated the T-DNA insertion position labeled with the Salk number. RT-PCR results exhibited that the fragment of *knat3* and *knat7* were not amplified in the corresponding mutants compared with WT (C), and ACT2 was used as an internal reference gene. The height of 6-week-old WT, *knat3*, *knat7*, and *knat3 knat7* were shown (D), Bar=5cm. Compared with the WT, there was no significant difference in the height of *knat3* and *knat7*, but the height of *knat3 knat7* was significantly shorter at the same stages (E). Data are mean with standard deviation of 10 plants. *** indicates a significant difference at $P < 0.01$ compared to wild-type plants, *t*-test. Complementation of *KNAT3* and *KNAT7* can rescue the height of *knat3 knat7* (F).

Figure 3. The *knat3 knat7* double mutant shows severe irregular xylem.

(A) to (D) are cross-sections of 6-week-old *Arabidopsis* base stems stained with phloroglucinol labeled WT (A), *knat3* (B), *knat7* (C), *knat3 knat7* (D). The upper panel shows the interfascicular fiber structure, and the lower panel shows the xylem tissue. Bar=20μm. (E) to (G) are cell wall thickness of different cells vessel cell (E), Xylary fiber cell (F) and Interfascicular fiber cell (G). Data are mean with standard deviation of 50 cell wall thicknesses. * indicates a significant difference at $P < 0.05$ compared to wild-type plants, ** indicates a significant difference at $P < 0.01$ compared to wild-type plants, *t*-test. (H) is cross sections of complementation plant by over-expressed *KNAT3* and *KNAT7* in *knat3 knat7* double mutant.

Figure 4. Lignin content and Mäule staining of WT, *knat3*, *knat7* and *knat3 knat7*.

Percentage content of acid-soluble lignin (A), acid-insoluble lignin (B) and total lignin (C) in the main stem of 8-week-old plants. Three biological replicates were included, and the significance analysis was based on student's *t*-test. * showed a significant difference at $P < 0.05$ compared to WT plants. (D) to (G) Cross-sections form the bases 6-week-old stem with Mäule staining, it can be observed that *knat3 knat7* stained with yellow-brown, comparing with WT red, Bar=20 μm. (H) Aromatic regions of 2D ^{13}C–^{1}H correlation (HSQC) spectra from cell wall gels from various samples in DMSO-d_6/pyridine-d_5 (4 : 1). The data showed that S lignin decreased and G-lignin increased in *knat3 knat7*. (I) Chemical formulas in different colors correspond to the color of different components (H).

Figure 5. S-lignin synthesis gene *F5H* was down-regulated.

(A) RNA-seq data showed the expression changes of lignin pathway gene. Red means up-regulation, green means down-regulation, purple means no change. The results were based on the difference of multiple Fold Change $\geqslant 2$ and the error rate FDR < 0.01 as the screening criterion. (B) qRT-PCR was used to detect the relative

expression of lignin metabolic pathway genes between WT and *knat3knat7* mutant. *PAL* (Phenylalanine Ammonia Lyase), *C4H* (Cinnamate 4-Hydroxylase), *4CL* (4-Coumarate CoA Ligase), *C3H* (Coumaroyl Shikimate 3'-Hydroxylase), *CAD* (Cinnamyl Alcohol Dehydrogenase), *F5H* (Ferulate 5-Hydroxylase). The expression level of each gene in the WT was "1", *EF1α* was used as an internal reference, and the error bar represented the standard deviation of 3 biological repetitions and 4 technical repetitions.

Figure 6. KNAT3 and KNAT7 can form dimer to activate *F5H* expression.

(A) Schematic representation of the transcriptional activation reporter and effector system. (B) The activation was carried out by adding different reporters and effectors to the Arabidopsis protoplasts, and the ratio of LUC and REN in the CaMV35S’-empty cells with only repoters control was "1". Column height indicates the mean ± standard deviation of the relative LUC/REN ratio with three biological replicates, n = 4, *P <0.05, **P <0.01; student's *t*-test. (C) Yeast one-hybrid assay detects KNAT3 and KNAT7 binding with the F5H promoter. Positive binding will show blue after the X-gal was added. As a negative control (AD), KNAT3 and KNAT7 cannot directly bind to the F5H promoter. (D and E) the interaction of KNAT3 and KNAT7 proteins was examined in yeast cells, KNAT3 CDS and GAL4 DNA-binding region (DBD) fused as a bait protein, GAL4 transcriptional activation region (AD) fused with KNAT3 or KNAT7 protein was used as prey (D), or the opposite of bait and prey (E). After transformation, the yeast was spotted on SD-Leu-Trp (-2) medium and SD-Leu-Trp-His (-3) screening medium containing 2.5 mm 3AT, and AD was used as a negative control. KNAT7 and KNAT3 can form homodimers and heterodimers. (F) KNAT3 and KNAT7 interact in plants, and the positions of the four corners represent different combinations of transformation. Only mixture of KNAT3 and KNAT7 proteins by split luciferase complementation experiments show fluorescent.

Figure 7. KNAT3/7 interact with NST1/NST2 proteins.

(A) KNAT3 and NST1/NST2 proteins interact by yeast two-hybrid, KNAT3 CDS and GAL4 DNA-binding region (DBD) fusion as bait protein, GAL4 transcriptional activation region (AD) fused with NST1/NST2/SND1 protein as prey. The transformed yeast was spotted in SD-Leu-Trp (-2) medium and SD-Leu-Trp-His (-3) with 2.5 mm 3AT, and AD was used as a negative control. (B) KNAT7 cannot interact with NST1/NST2/SND1 in yeast cells. (C) and (D) KNAT3 and NST1/NST2 interact in plants, the positions of the four corners represent different combinations of constructs for transformation. (E) Co-immunoprecipitation assay of KNAT3-HA and NST1/2-FLAG. The proteins were immunoprecipitated with anti-FLAG antibody, and then probed with anti-HA antibody. (F) Transcriptional activation experiments were tested by reporters combining with different effectors in Arabidopsis protoplasts. CaMV35S’-empty with only reporter was regarded as control with the ratio of LUC and REN as "1" for normalization. Column height indicates the mean ± standard deviation of the relative LUC/REN ratio of each combination with three biological replicates, n = 4. ** P <0.01; Student's *t*-test.

Figure 8. The hypothesis model of KNAT3/KNAT7 Synergistically regulate S-lignin biosynthesis.

KNAT3 and KNAT7 can form heterodimer. The proteins MYB75, OFP4 and BLH6 were reported as negative regulators interacting with KNAT7 to repress F5H in some cell types and the proteins NST1/2 were reported as positive regulator interacting with KNAT3 to activate F5H in specific cell.

Figure 1

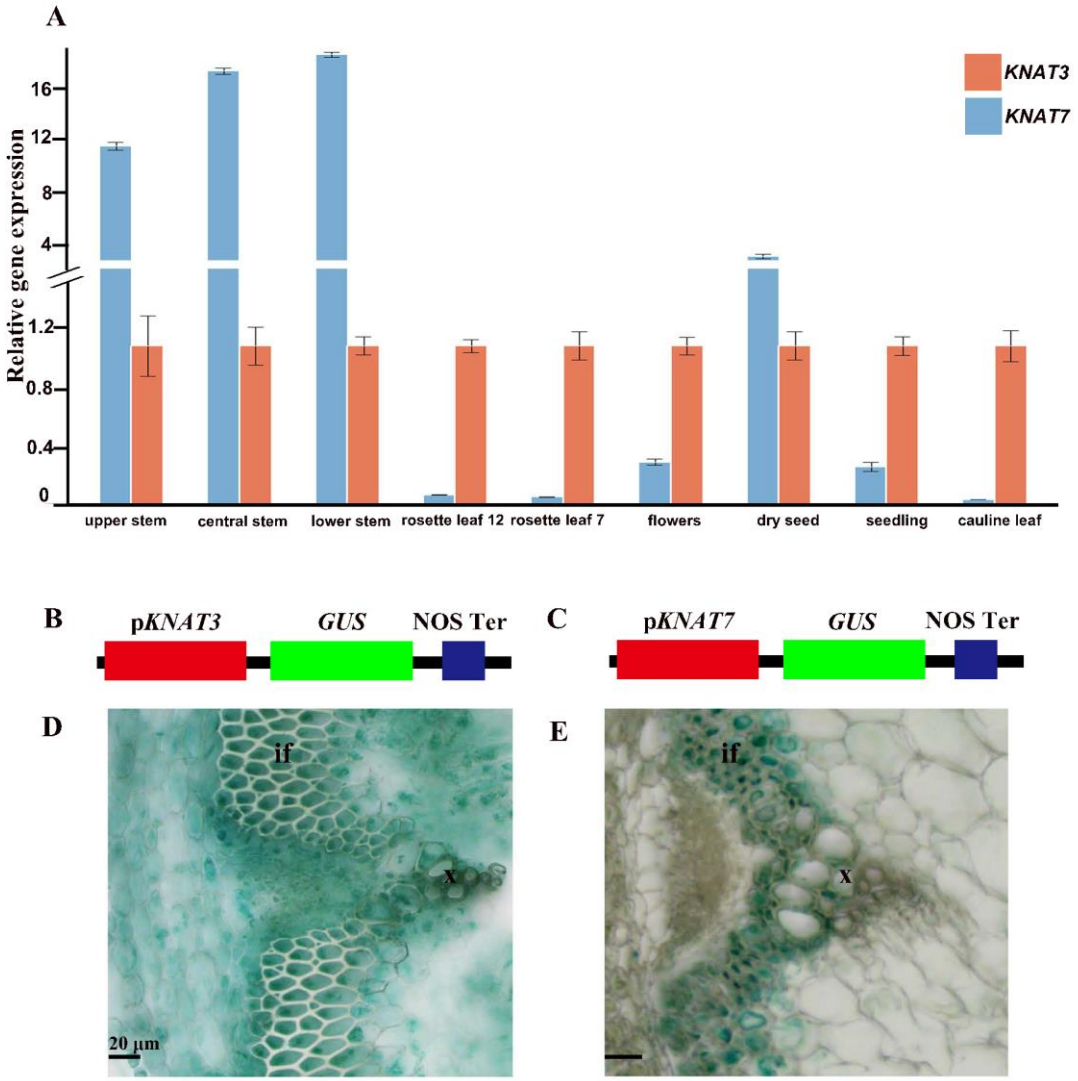

Figure 2

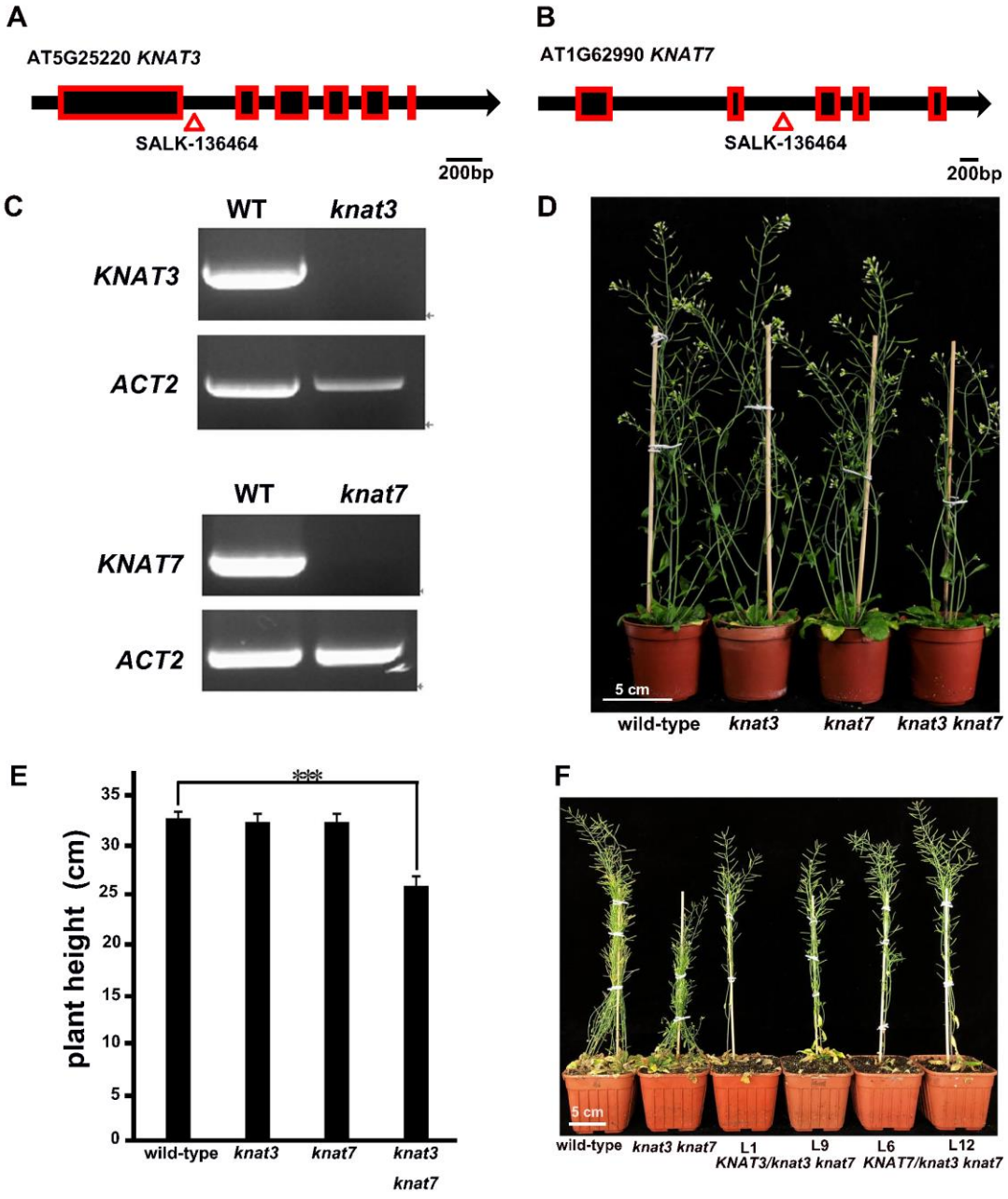

Figure 3

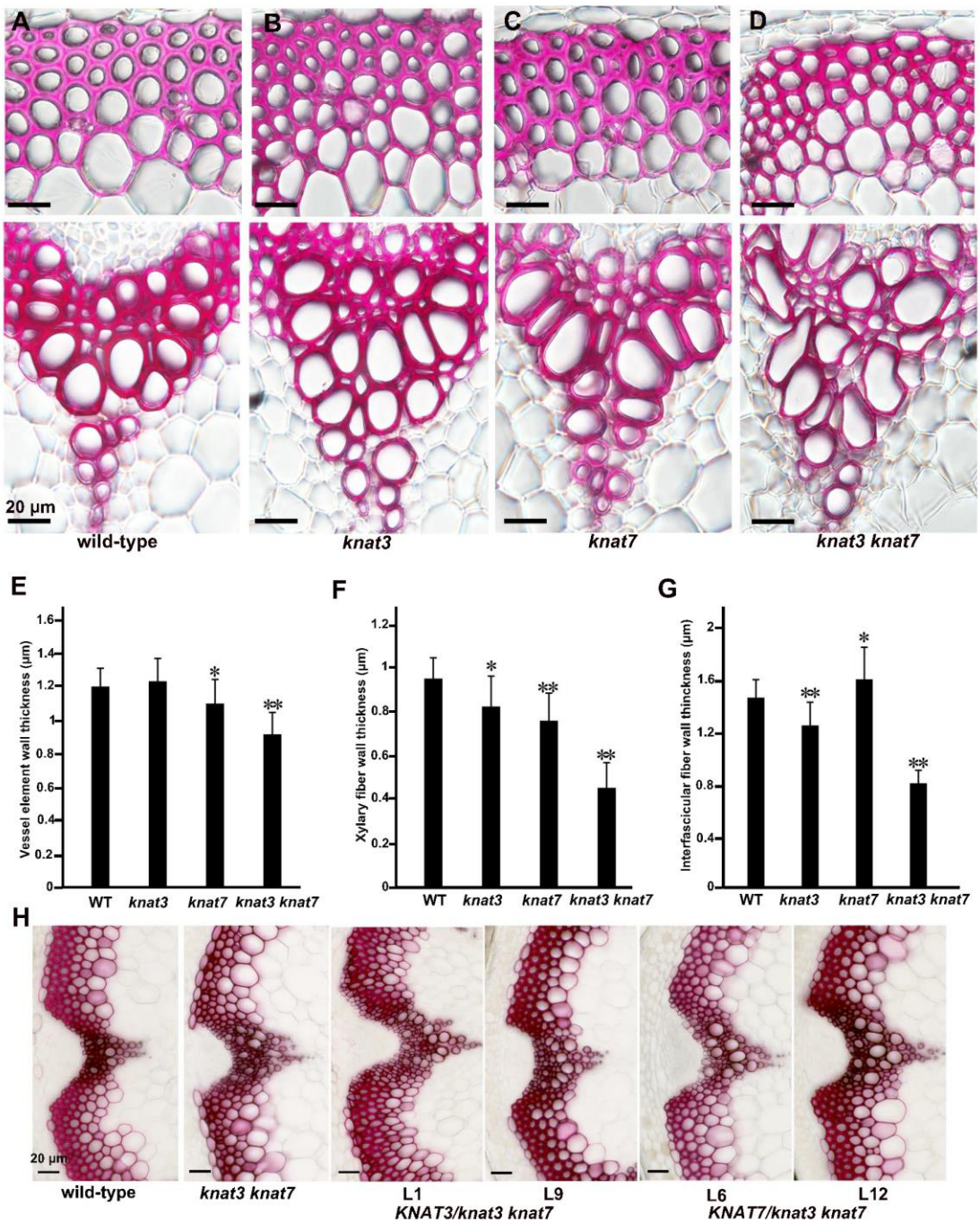

Figure 4

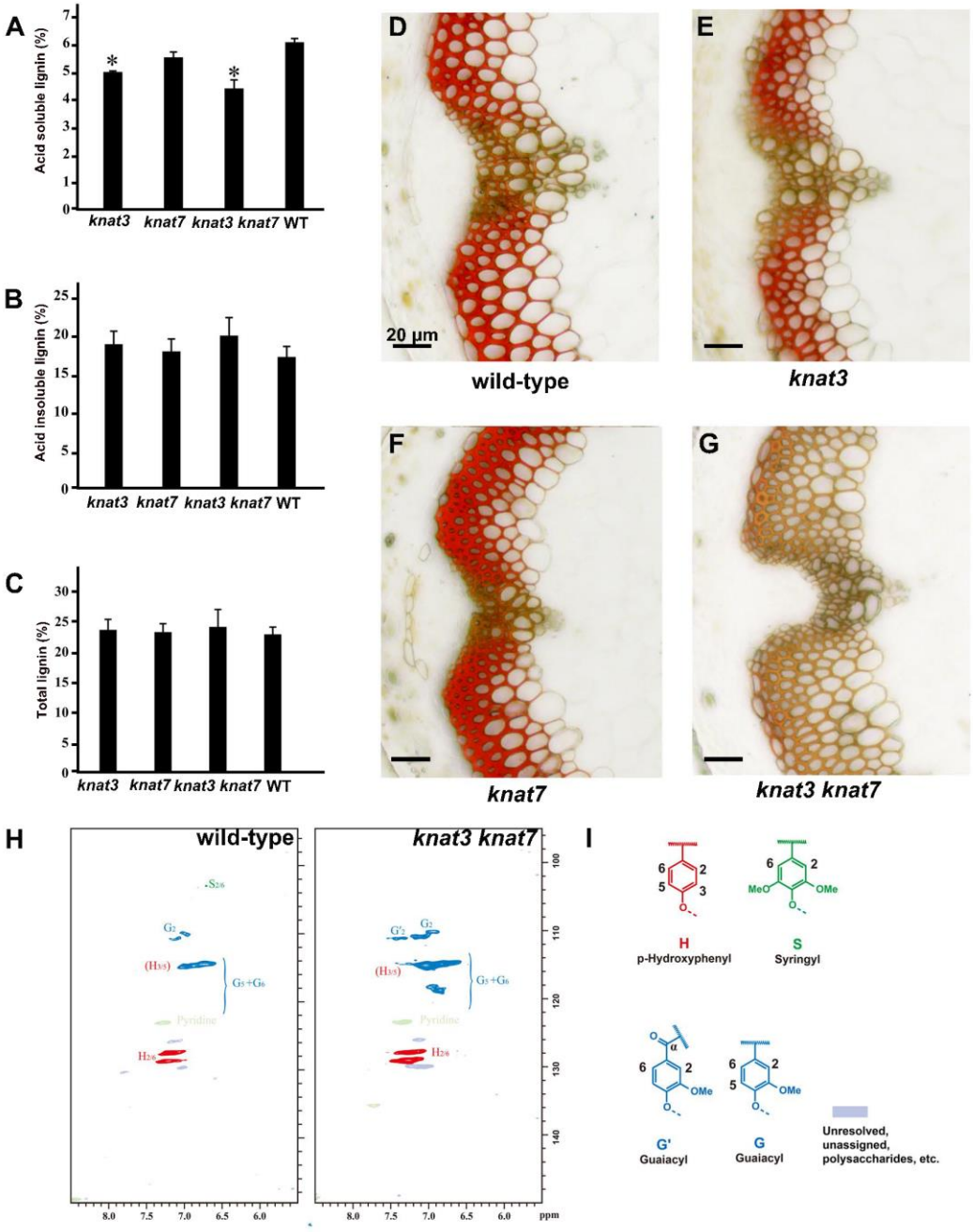

Figure 5

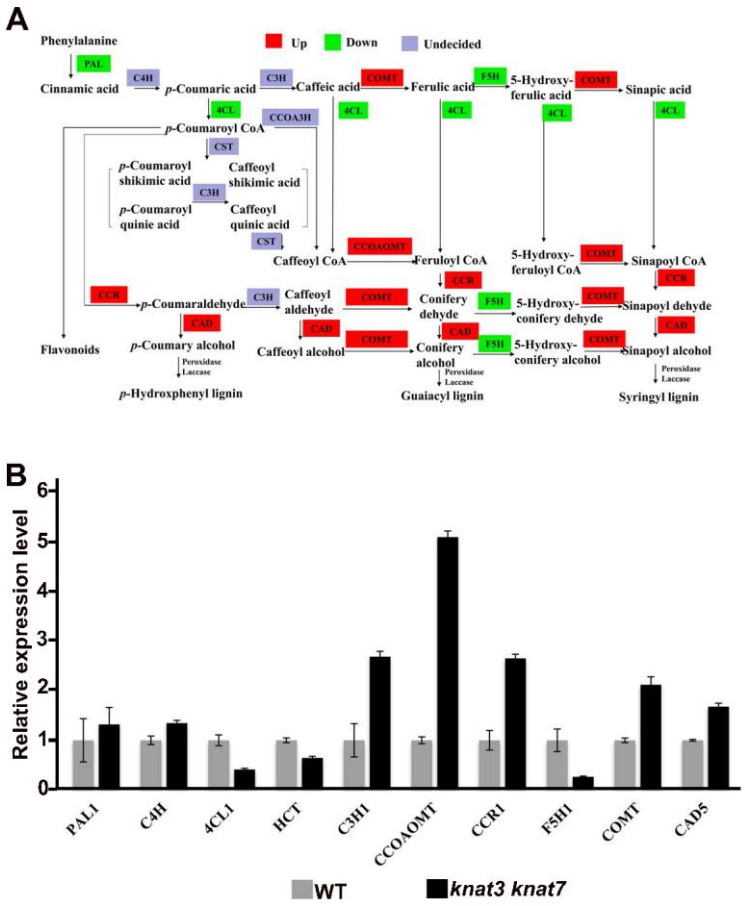

Figure 6

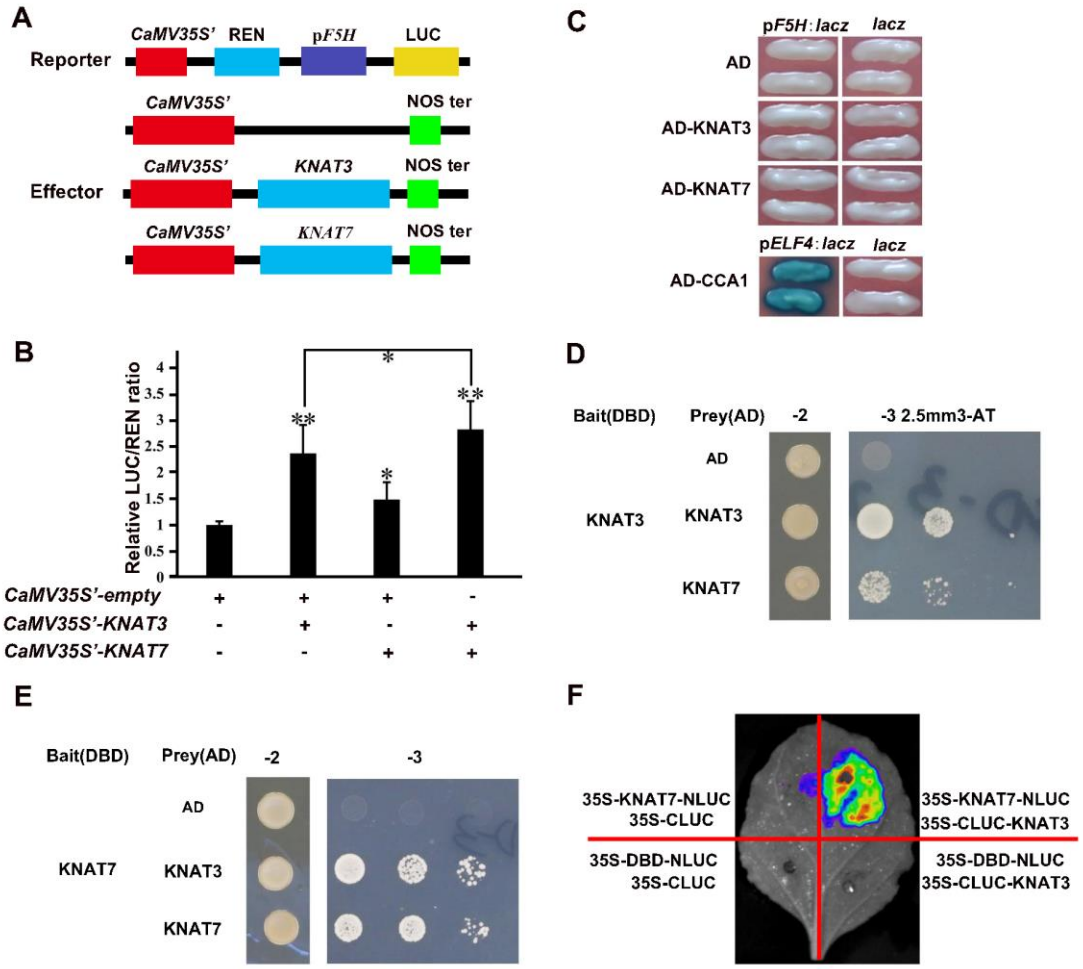

Figure 7

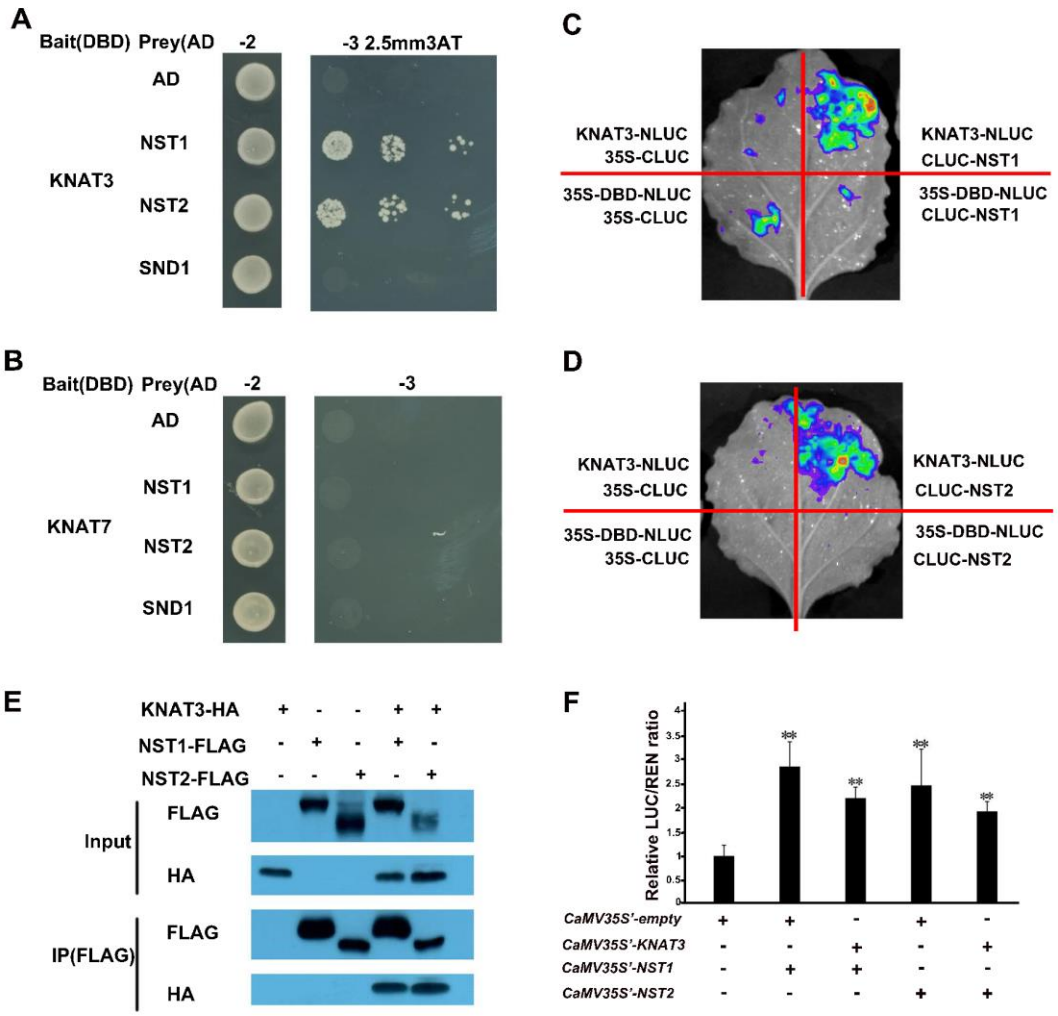

Figure 8